Concept and setup for intraoperative imaging of tumorous tissue via Attenuated Total Reflection spectrosocopy with Quantum Cascade Lasers

Florian B. Geiger*[ab], Martin Koerdel[b], Anton Schick[b], Axel Heimann[c], Kaspar Matiasek[d] and Alois M. Herkommer[a]

[a]Institute of Applied Optics, University of Stuttgart, Pfaffenwaldring 9, 70569 Stuttgart, Germany; [b]Siemens AG Corporate Research (CT RTC SET INT-DE), Otto-Hahn-Ring 6, 81739 Munich, Germany; [c]Institute for Neurosurgical Pathophysiology, University Medical Center of the Johannes Gutenberg-University Mainz, Langenbeckstr. 1, Mainz 55131, Germany; [d]Section of Clinical and Comparative Neuropathology at the Centre for Veterinary Clinical Medicine, Ludwig Maximilians University, Veterinaerstrasse. 13, 80539 Munich, Germany

ABSTRACT

A major challenge in tumor surgery is the differentiation between normal and malignant tissue. Since an incompletely resected tumor easily leads to recidivism, the gold standard is to remove malignant tissue with a sufficient safety margin and send it to pathology for examination with patho-histological techniques (rapid section diagnosis). This approach, however, exhibits several disadvantages: The removal of additional tissue (safety margin) means additional stress to the patient; the correct interpretation of proper tumor excision relies on the pathologist's experience and the waiting time between resection and pathological result can be more than 45 minutes. This last aspect implies unnecessary occupation of cost-intensive operating room staff as well as longer anesthesia for the patient. Various research groups state that hyperspectral imaging in the mid-infrared, especially in the so called "fingerprint region", allows spatially resolved discrimination between normal and malignant tissue. All these experiments, though, took place in a laboratory environment and were conducted on dried, ex vivo tissue and on a microscopic scale. It is therefore our aim to develop a system incorporating the following properties: Intraoperatively and in vivo applicable, measurement time shorter than one minute, based on mid infrared spectroscopy, providing both spectral and spatial information and no use of external fluorescence markers. Theoretical assessment of different concepts and experimental studies show that a setup based on a tunable Quantum Cascade Laser and Attenuated Total Reflection seems feasible for in vivo tissue discrimination via imaging. This is confirmed by experiments with a first demonstrator.

Keywords: Tissue Differentiation, Tumor Recognition, Mid Infrared (MIR) Spectroscopy, Quantum Cascade Laser, Fourier Transform Infrared Spectroscopy (FTIR), Attenuated Total Reflection (ATR), Hyperspectral Imaging.

1. INTRODUCTION

1.1 Challenge

Research shows that partial tumor resection results in higher recurrence than full resection.[1–6] Therefore, one of the main goals during surgery is to remove malign tissue completely.[2,4,7–10] In some cases this can be achieved by additionally removing healthy tissue enclosing the tumor (safety margins).[3,7,11] Removing healthy tissue, however, is especially problematic in regions of highly functional tissue, e.g. the brain. In order to reduce negative impact on body functions, safety margins thus have to be kept as small as possible, if they can be implemented at all.[2,6,9,12,13]

A clear identification of tumor excision borders is therefore needed. This poses a challenge for surgeons, because

*florian.geiger.ext@siemens.com; phone +49 89 636 634 283

Medical Imaging 2015: Physics of Medical Imaging, edited by Christoph Hoeschen, Despina Kontos,
Proc. of SPIE Vol. 9412, 94125F · © 2015 SPIE · CCC code: 1605-7422/15/$18 · doi: 10.1117/12.2081837

it is hard and sometimes impossible to clearly differentiate between normal and tumorous tissue with human senses alone.[14]
State of the art to ensure complete resection is the examination of removed tissue by histopathological methods.[15,16] This approach includes sending the tissue to pathology right after removal, cutting and staining thin tissue sections and observing color and morphology with an optical brightfield microscope. Results are obtained after 20 min at the earliest.[10,15] The main restriction of this approach is spatial and temporal separation of excision and diagnosis. This method therefore does not help to minimize safety margins or surgery time.
Other possibilities to differentiate between normal and tumorous tissue are known ways of classical medical imaging such as ultrasound (US), magnetic resonance imaging (MRI), computed tomography (CT) and positron emission tomography (PET). Restrictions for in vivo use are poor image quality (US), high costs (MRI, CT, PET), space problems (MRI, CT, PET) and ionizing radiation exposure (CT, PET).[10,17,18]

1.2 State of research

Tumor recognition via mid infrared (MIR) spectroscopy seems a promising way to overcome the aforementioned problems. There are two basic approaches in this field: Firstly, the implementation of non imaging cancer recognition systems that aim for in vivo use[19–29] and secondly imaging systems for ex vivo use.[30–51] The first approach is usually either realized as an endoscope to do *single point* in vivo diagnosis or as a spectrometer placed in the operating room to do ex vivo diagnosis of untreated and freshly resected tissue. The second approach uses hyperspectral imaging to produce maps of dried tissue slices that show areas of different tissue types in the form of false color maps. This is done in a laboratory separated from the operating room.
The combination of both approaches would lead to an imaging system for in vivo use that could help surgeons to differentiate between tumorous and healthy tissue intraoperatively.[21] Spatial and temporal separation between resection and diagnosis would be eliminated, resulting in reduced safety margins and surgery time.

1.3 Suggested approach

A system offering the aforementioned qualities, must feature the following properties:

- In vivo means watery and undried environment. The system therefore must be able to produce strong signals in spite of strong water absorption in the mid infrared.
- In vivo also means patient movement, therefore relative movement between imaging device and patient has to be eliminated.
- Imaging time should be as fast as possible (less than a minute) to ensure acceptance of surgeons.
- The image size should have the dimension of the size of a tumor, that is the image size should be in the range of square millimeters to square centimeters.
- High spatial resolution is not required, because resolution does not have to be higher than a surgeon can dissect. Spatial resolution of about 1 mm should therefore be sufficient.
- Using no fluorescence markers reduces negative impact on the patient as well as problems with device certification.

Doing MIR spectroscopy of undried tissue samples is said to be difficult, because water signals in the MIR are very strong compared to tissue signals.[9,26,52,53] There is, however, a region between approximately 1500 cm^{-1} and 1000 cm^{-1}, in which reasonable spectra acquisition of undried tissue seems viable. This is indicated by the following three aspects: Firstly, this region covers much of the fingerprint region and therefore contains a huge amount of spectroscopic information. Secondly, water absorption there is low compared to its surroundings and thirdly, water absorption is comparatively constant, as it is shown in Fig. 1.

In spectroscopy, radiation can be brought into contact with the sample either in transmission or reflection mode. Due to tissue thickness, the only way to do in vivo spectroscopy is using reflection mode. There are two routine reflection measurement modes for working with biological tissue: Diffuse reflection (DR) and Attenuated

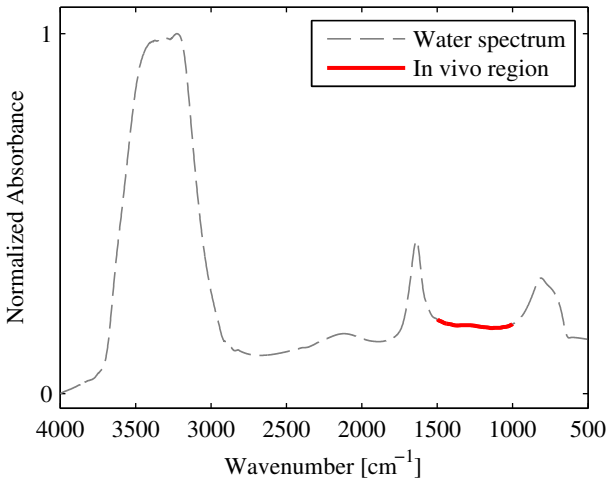

Figure 1. FTIR spectrum of water; region of relatively constant and weak water absorption is highlighted.

Total Reflection (ATR).[23] DR describes the reemerging of scattered photons from the upper surface of a sample.[54] This happens if tissue is illuminated *directly*. In case of ATR, however, total internal reflection (TIR), that is *specular* reflection, is established at the interface of an internal reflecting element and the sample, e.g. tissue. TIR implies an exponentially declining wave penetrating the sample a few wavelengths. This *evanescent wave* can be partially absorbed by the sample and can therefore be used for spectroscopy.[55–57]
It was shown that a water film of only 2 µm on undried tissue leads to an almost complete elimination of tissue bands in case of diffuse reflection.[23] Using ATR, however, allows reducing the water layer thickness on a tissue's surface by pressing the internal reflection element (e.g. a diamond crystal) onto the sample. This is shown in Fig. 2: While there still is a PMMA signal despite the water in case of ATR, water eliminates the PMMA signal completely in case of DR.
Thus, spectra of wet tissue in the above-mentioned region of 1500 cm^{-1} to 1000 cm^{-1} should show spectral information of water overlaid with spectral information of tissue, given that water reduction by using ATR is adopted. The more contact pressure is applied, the less water should be detected and the stronger the tissue signal will be. Due to the constant water absorption in the mentioned region, spectral information should be easier extractable than in areas of strong and varying water absorption.
Besides minimizing the water layer, contact between crystal and tissue reduces relative movement between sensor and patient during acquisition, which is a second crucial benefit.

FTIR spectroscopy is regarded as state of the art concerning spectroscopy of biological tissue, although broadly tunable Quantum Cascade Lasers (QCLs) are becoming more and more popular in biomedical applications.[58–61] Advantages of QCLs compared to FTIR spectrometers are their higher spectral power and better beam quality as well as lower complexity and maintenance effort. A drawback on the other hand is their lower spectral bandwidth. Commercially available QCL systems have a tuning range of up to 1000 cm^{-1}, while FTIR spectrometers in the MIR usually have about four times as much. Taking the above-mentioned region between 1500 cm^{-1} and 1000 cm^{-1} into consideration, however, the bandwidth of QCLs is sufficient.
In this study we present a novel hyperspectral imaging setup in order to answer two questions:

- Can reasonable spectra of undried tumorous tissue be generated with a single reflection ATR crystal system? The number of reflections is roughly proportional to the signal strength. Therefore, single reflection leads to an accordingly lower absorption signal than multiple reflections applied by others.[19,21,22,24,26] Single reflection is, however, necessary for imaging to preserve spatial specificity.[62]
- Does a simple QCL setup produce imaging results similar to a commercial FTIR spectrometer?

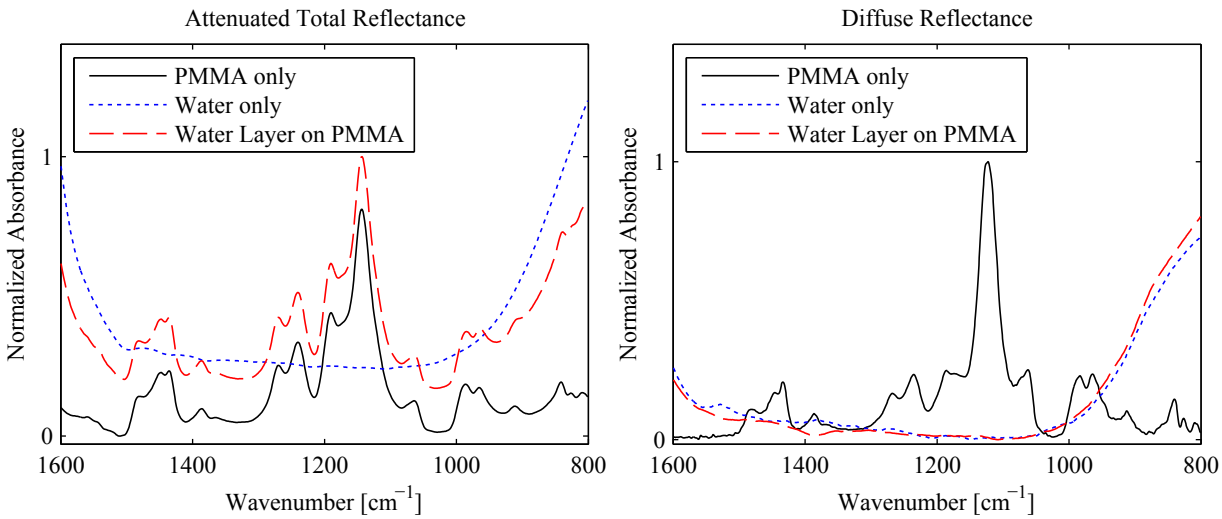

Figure 2. Left: Pressing the Attenuated Total Reflection crystal onto the PMMA section reduces the water film thickness and therefore the spectral influence of water. This results in a spectrum consisting of spectral information of both PMMA and water. Right: In case of using Diffuse Reflectance, water on the PMMA section results in elimination of the PMMA signal. Shown Diffuse Reflectance spectra were transformed by Kramers-Kronig relations.

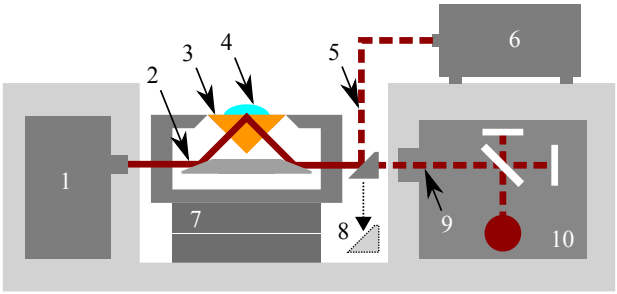

Figure 3. Overview of the experimental setup; (1) MCT detector, (2) radiation of QCL or FTIR, (3) ATR crystal, (4) Sample, (5) QCL radiation, (6) QCL, (7) x-y-stage, (8) deflection mirror to choose between QCL and FTIR, (9) FTIR radiation, (10) FTIR radiation source and interferometer.

2. MATERIAL AND METHODS

2.1 Setups

2.1.1 Scanning ATR Device

Due to the aforementioned requirements, our setup had to feature the following properties:

- Image size of approximately $8 \times 8\,\mathrm{mm}^2$.
- Spatial resolution of approximately 1 mm.
- An ATR crystal to minimize water layer thickness.
- Possibility to adjust contact pressure.
- A basin to work with wet samples and fluids.

Furthermore, as we wanted to compare FTIR and QCL based systems, our device had to be suitable for both FTIR and QCL setups without time-consuming alterations.

Fig. 4 shows the realization of the setup. We implemented a scanning system combined with the nitrogen-cooled single detector of our FTIR spectrometer, which is described below. A rectangular zinc selenide prism

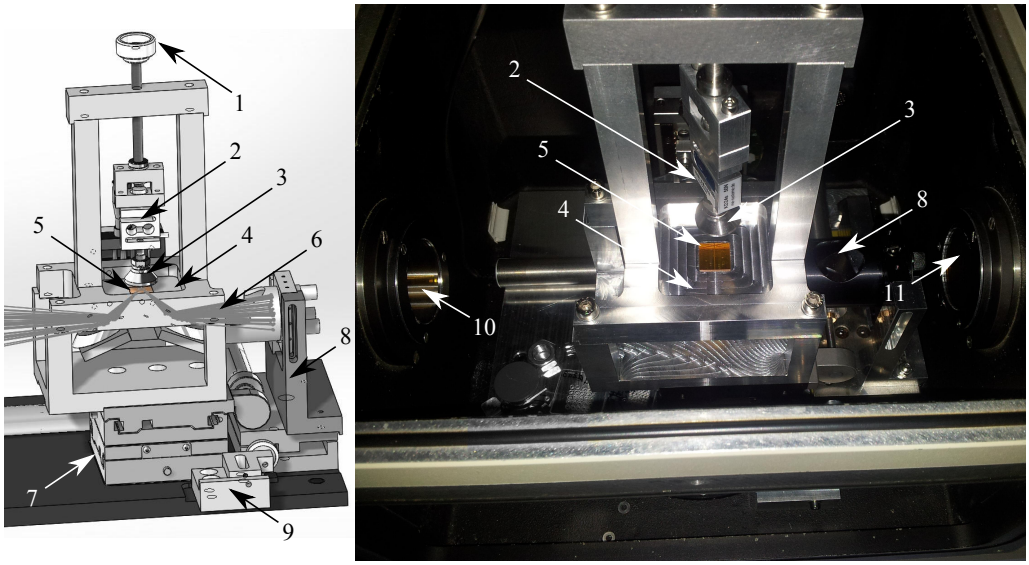

Figure 4. Novel setup for imaging of freshly resected tissue; (1) screw mechanism for applying contact pressure, (2) force sensor, (3) swivel foot, (4) basin, (5) ATR crystal, (6) optical path, (7) x-y-stage, (8) movable deflection mirror unit, (9) magnet for setting mirror to QCL position, (10) radiation exit (detector chamber), (11) FTIR radiation entrance.

with a base area of $15 \times 15\,\mathrm{mm}^2$ is used as a single reflection ATR element. It is embedded in a basin that can be filled with fluid to simulate "in vivo" environment. Above the crystal is a screw mechanism with a built-in force sensor to apply well-defined contact pressure between sample and crystal. A swivel foot ensures balanced contact pressure on the sample. The crystal can be moved by an automated x-y-stage while the light path is fixed. This generates spatial resolution by scanning; the image size is $8 \times 8\,\mathrm{mm}^2$. Mapping was done at $8 \times 8 = 64$ locations, separated by a spatial distance of 1 mm in both directions. To compare FTIR and QCL spectroscopy without changing the sample, a movable deflection mirror with a focus length of 100 mm allows selecting between the FTIR and the QCL input beam. The mirror is mounted on a linear stage that can be fixed in two different positions using a magnet. This allows switching between the FTIR and the QCL setup within a few seconds, since both FTIR and QCL systems use the same detector, as described below (see Fig. 3).
For the x-y-stage control we used self written software based on Microsoft batch files that could communicate with the control software of our FTIR and QCL systems.

2.1.2 FTIR Setup

For the FTIR experiments we used a Bruker IFS66v spectrometer together with a liquid nitrogen cooled single MCT detector. The ATR setup described above was put into the sample chamber of the spectrometer, which is shown in the photograph on the right of Fig. 4. To use the FTIR radiation, the deflection mirror has to be set to the FTIR measurement position. For the spectrometer control we used Macros written with OPUS Software by Bruker. FTIR spectra were recorded between 4000 cm^{-1} and 400 cm^{-1} with a resolution of 4 cm^{-1}; 30 spectra were co-added. In order to establish spatial resolution, we used an aperture size of 1 mm.

2.1.3 QCL Setup

The Quantum Cascade Laser we used was an Übertuner 8 from Daylight Solutions, emitting linearly polarized radiation in the spectral range between roughly 1310 cm^{-1} and 1150 cm^{-1} at 100 kHz pulse repetition rate and 500 ns pulse width. For the experiment, the laser was placed on top of the FTIR spectrometer. Its beam was deflected into the sample chamber of the FTIR spectrometer from above and then directed onto the crystal of the scanning ATR device by the movable deflecting mirror setup described above (see Fig. 3). The QCL setup incorporated the MCT detector of the FTIR spectrometer; the signal was recorded directly from the preamplifier by a digital oscilloscope. Because the QCL's emitted radiation power was above the detector's saturation level, we used a polarizer for damping the beam. The data was saved by a digital oscilloscope; data analysis was done

via Matlab.
QCL spectra were recorded in 4 cm^{-1} steps. For one 4 cm^{-1} step we co-added the pulse maxima of 20 pulses.

2.2 Experiments

2.2.1 Spectra of undried tissue via FTIR

To show the ability of our single reflection ATR device to generate spectra of undried tumorous tissue, we used two different tumorous tissue sections:

- A tumorous dog brain section, shown in the photograph on the left of Fig. 6. The tissue was resected at the Section of Clinical and Comparative Neuropathology (Centre for Veterinary Clinical Medicine, Ludwig Maximilians University) from a 7 year old mongrel dog presenting with non-specific forebrain signs. Magnetic resonance imaging revealed a left lateral ventricle mass lesion. The owners elected euthanasia and agreed to full postmortem examination. On brain trimming a haemorrhagic intraventriclar mass was seen, histology of which was consistent with an exophytic plexus papilloma. After resection, the tumorous tissue was kept in an airtight container to prevent drying. For the spectroscopic experiment a few hours after resection, the tissue was put onto the wetted ATR crystal. "Wetted" here means that a few drops of water were placed on the crystal to prevent tissue drying during the experiment.
- A tumorous rat brain section, shown in the photograph on the right of Fig. 6. To receive this tumorous tissue, 7 µl of C6 glioma cell suspension (4×10^6 cells) were implanted stereotactically into the left parietal cortex of an adult male Wistar rat (Charles River Wiga, Sulzfeld, Germany) by a Hamilaton syringe (burr-hole trephination 1.2 mm Ø). The tumor was allowed to grow for 7 days. The animal was bred and kept at an animal facility in a temperature-controlled environment on a 12-hour light/dark cycle (diet and water ad libitum). The rat was anesthetized by Medetomidin (0.4 mg/kg b.w.) and Ketamin (75 mg/kg b.w.). Analgesie was performed with Tramadol (30 mg/kg b.w.). The rat experiment was performed at the Institute for Neurosurgical Pathophysiology (Medical Center, Johannes Gutenberg-University Mainz) in accordance with national and international guidelines and were approved by the Governmental Animal Care and Use Committee. After resection, the brain section remained in a PFA solution (4%, buffered, pH 7.4) until the spectral experiment. The tissue section was taken out of the PFA solution and directly put onto the crystal for measurement. The tumor was located within the highlighted range of measurement in Fig. 6.

Contact pressure between samples and crystal was approximately 1 N/cm^2.
Absorbance spectra were calculated according to Eq. (1). Background spectra were taken with water (dog) and PFA solution (mouse) covering the ATR crystal. The corresponding fluid being part of both sample (moist tissue) and background spectrum reduces the fluid's influence on the absorbance spectrum due to canceling [see Eq. (1)].
The ATR crystal was cleaned with water and ethanol before changing or moving the sample.

$$Absorbance = -log_{10}\left(\frac{Sample\,Spectrum}{Background\,Spectrum}\right) \tag{1}$$

2.2.2 Hyperspectral imaging of Polymethylmethacrylate (PMMA) via FTIR and QCL

To compare both QCL and FTIR setups in matters of ATR imaging, we used a plate made of PMMA. It features two holes and a groove (see Fig. 7) and is 1 mm thick. The plate was used, because it was expected to lead to unambiguous results. The reason for this is that the plate does not change its spectral characteristics over time, in contrast to e.g. drying tissue. Furthermore, PMMA shows higher absorption than tissue and the holes and groove are expected to be clearly recognizable in a hyperspectral image. The plate was pressed onto the ATR crystal with a pressure of about 30 N/cm^2.
Mapping the plate results in two different kinds of spectra: At locations of holes and grooves, that is "empty space", absorbance is a zero baseline plus noise; locations of PMMA naturally show PMMA spectra and transition regions show PMMA spectra, too, but with less intensity. Thus, we used the intensity of only one PMMA

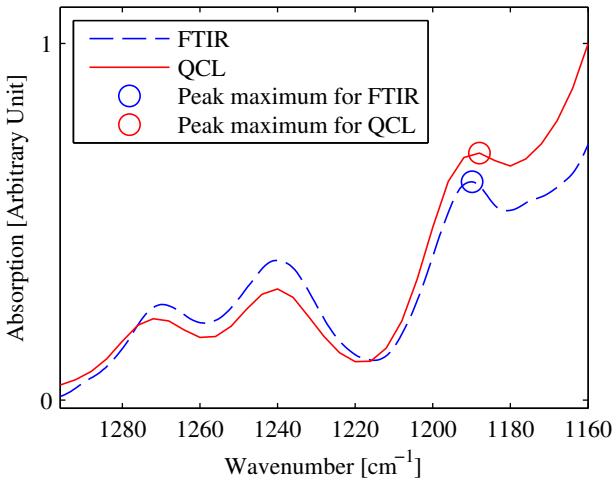

Figure 5. FTIR and QCL spectra of PMMA; both spectra were generated using the single reflection ATR setup; peak maxima used for imaging are highlighted.

absorbance peak at around 1190 cm^{-1} to differentiate between PMMA, no PMMA and transitions. The peaks at about 1190 cm^{-1} are shown in Fig. 5. In the resulting grayscale images, each absorbance intensity of the maximum at 1190 cm^{-1} corresponds to a grayscale value, so that black pixels represent high absorbance and white pixels low absorbance.
Background spectra were recorded without a sample on the crystal. Absorbance was calculated according to Eq. (1). Mapping of all 64 pixels took about 20 min for both QCL and FTIR setups.

3. RESULTS AND DISCUSSION

3.1 Spectra of undried tumorous tissue via FTIR

Fig. 6 presents spectra of tumorous dog and rat brain sections. The results show that the generation of reasonable spectra of undried tissue is feasible using single reflection ATR spectroscopy. The spectra clearly show the following typical features of tissue spectra resembling those from literature:[63–65]

- Amide I at around 1645 cm^{-1}.
- Amide II at around 1550 cm^{-1}.
- Asymmetric CH_3 bending modes of methyl groups in proteins and CH_3 bending modes of membran lipids at around 1460 cm^{-1}.
- Symmetric CH_3 bending modes of methyl groups in proteins at around 1400 cm^{-1}.
- Asymmetric stretching modes of phosphodiester groups at around 1240 cm^{-1}.
- Symmetric stretching modes of phosphodiester groups at around 1080 cm^{-1}.

The experiments therefore show that generating spectra of undried tissue by a potentially in vivo and imaging (single reflection) technique is feasible.

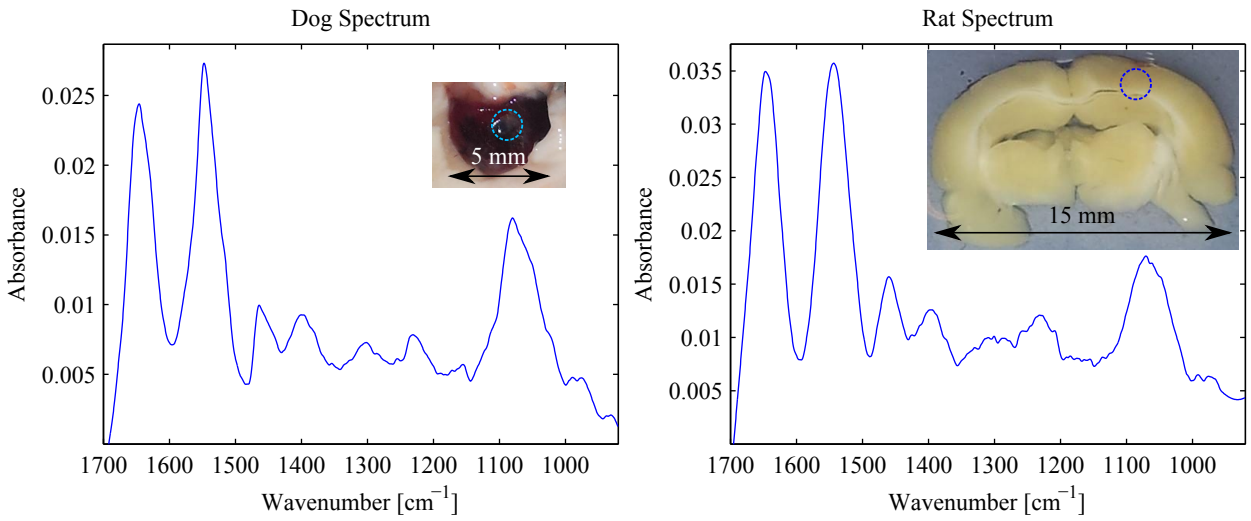

Figure 6. Spectra of undried tumorous tissue sections of dog (left) and rat (right). Spectral features resemble those from literature. Photographs show corresponding samples and range of measurement (dashed lines), i.e. the approximate spot size of the infrared radiation on the tissue.

3.2 Hyperspectral imaging of PMMA via FTIR and QCL

Fig. 7 shows the mapping capabilities of both FTIR and QCL setups. Although the sections do not overlap perfectly, which is due to a slight difference in optical paths, one can clearly see the comparability. This is the case, although the QCL setup is significantly less complex than the FTIR device. Furthermore, the QCL setup is much better suited for an intraoperatively used application due to the following reasons:

- The QCL setup is much smaller in size and weight, which is favorable if it comes to an intraoperatively used hand-held system.
- It does not have to heat up like an FTIR spectrometer for more than 30 min and can therefore be used without long waiting periods.
- It does not incorporate delicate parts such as an interferometer, which is why maintenance should be easier.
- Due to the high spectral power of the laser, there is potentially no need for liquid detector cooling. Therefore, time consuming filling of a detector's dewar as well as providing and handling liquid nitrogen within the operating room is not required.

In addition, due to better beam quality of QCLs compared to FTIR spectrometer light sources (Glowbars), QCL spectrometers have the potential to achieve much better spatial resolutions than FTIR setups. This is an important aspect, if higher resolution should be required in future setups.
Although producing comparable results in matters of spatial resolution, spectral sensitivity of the QCL setup was not yet as good as the FTIR spectrometer's. A major reason for this is laser intensity variation over time. To improve results in case of, compared to PMMA, low absorbing samples such as tissue, averaging over several measurements is one option. This, however, naturally takes accordingly more time, which is problematic in case of imaging tissue. The reason for this is that fresh tissue changes its spectral characteristics due to drying, if the measurement takes too long. Another option to improve results thus is to measure laser intensity variation using a second detector, which we implement in our next setup.

4. CONCLUSION

It was shown that generating spectra of undried tumorous tissue using single reflection ATR is feasible. Since single reflection ATR is a technique that can be used for imaging, those results show that differentiation of fresh

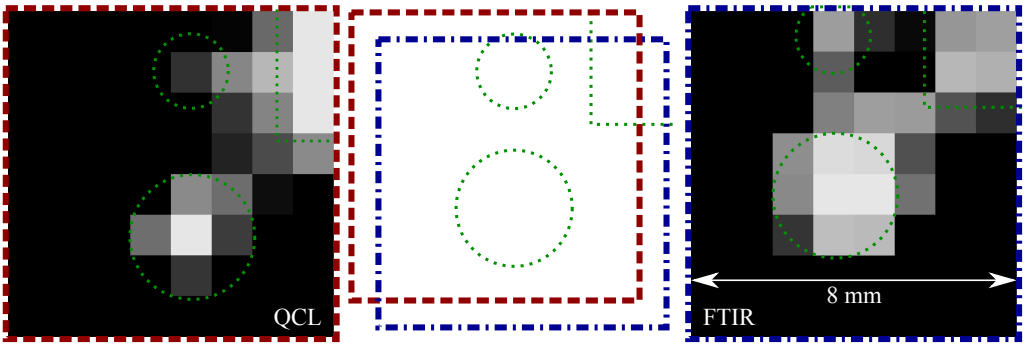

Figure 7. Grayscale images (QCL left, FTIR right), resulting from mapping of the PMMA section shown in the photograph (middle); Corresponding features are marked with dotted lines.

and undried tissue using hyperspectral imaging seems viable.

We furthermore showed that a setup incorporating a QCL and an ATR device seems the right choice for the long term objective to establish an in vivo tumor recognition system based on hyperspectral imaging. This is, because the QCL setup has the potential to produce imaging results similar to a commercial FTIR spectrometer, while it is at the same time smaller and simpler. Still, spectra recorded with the FTIR spectrometer are yet more sensitive. This, however, will likely change if a more sophisticated QCL setup will be used in thek future. One alternative to increase imaging speed is an upcoming generation of new QCLs that allow scanning of a few hundred wavenumbers within tens of milliseconds rather than seconds. To our knowledge, this is either achieved by microelectromechanical systems (MEMS) or oscillating gratings, depending on the manufacturer. Others use matrix detectors (Focal Plane Arrays, FPAs) to increase imaging time, though only for imaging of dried tissue in transmission mode.[60,61] Those FPAs, however, show significantly higher noise levels than corresponding single detectors. Since the use of ATR in our case, let alone single reflection ATR, leads to much lower absorbance, those types of FPAs do not seem an option for our use.

Besides improving the QCL setup, future work includes imaging of undried tumorous tissue. It should be mentioned here, that spectra of wet tissue will, of course, very likely never be as good as spectra of dried and sliced tissue. It is, however, not our aim to produce high quality spectra on a microscopic scale in order to replace tissue histopathology,[61] but to develop a tool that is able to highlight regions for resection. Such a device therefore does not have to be able to differentiate between normal and tumorous tissue without knowing anything about the patient's tissue characteristics, the specific cancer in question or cancer stage. It rather can be "calibrated" with the help of tissue that has been resected for diagnosis purposes before surgery. One could also think of calibration being done *during* surgery, using the spectra of regions that are clearly tumorous and clearly non tumorous in order to allow evaluation of transitions.

REFERENCES

[1] Mai, K., Yazdi, H., and Isotalo, P., "Resection margin status in lumpectomy specimens of infiltrating lobular carcinoma," *Breast Cancer Research and Treatment* **60**, 29–33 (March 2000).

[2] Lacroix, M., Abi-Said, D., Fourney, D., Gokaslan, Z., Shi, W., DeMonte, F., Lang, F., McCutcheon, I., Hassenbusch, S., Holland, E., Hess, K., Michael, C., Miller, D., and Sawaya, R., "A multivariate analysis of 416 patients with glioblastoma multiform: Prognosis, extent of resection, and survival," *J. of Neurosurgery* **95**, 190–198 (August 2001).

[3] Chagpar, A., Martin, R., Hagendoorn, L., Chao, C., and McMasters, K., "Lumpectomy margins are affected by tumor size and histologic subtype but not by biopsy technique," *The American J. of Surgery* **188**, 399–402 (October 2004).

[4] Kim, Y.-J., Bochem, N., Ketter, R., Henn, W., and Feiden, W., "Meningeome - multiparametrische risikostratifizierung und grading," *Pathologe* **29**, 428–433 (September 2008).

[5] Dener, C., Inan, A., Sen, M., and Demirci, S., "Interoperative frozen section for margin assessment in breast conserving energy," *Scandinavian J. of Surgery* **98**(1), 34–40 (2009).

[6] Stupp, R., Reni, M., Gatta, G., Mazzab, E., and Vecht, C., "Anaplastic astrocytoma in adults," *Critical Reviews in Oncology/Hematology* **63**, 72–80 (2007).

[7] Juhl, H., [*Chirurgie*], ch. 2, D. Henne-Bruns, B. Kremer, M. Dürig. 3. Auflage. Georg Thieme Verlag, Stuttgart (2008).

[8] Jacobs, L., "Positive margins: The challenge continues for breast surgeons," *Annals of Surgical Oncology* **15**, 1271–1272 (March 2008).

[9] Stelling, A., Salzer, S., Kirsch, M., Sobottka, S., Geiger, K., Koch, E., Schackert, G., and Steiner, G., "Intraoperative optical diagnostics with vibrational spectroscopy," *Analytical and Bioanalytical Chemistry* **400**, 2745–2753 (July 2011).

[10] Gajjar, K., Heppenstall, L., Pang, W., Ashton, K., Trevisan, J., Patel, I., Llabjani, V., Stringfellow, H., Martin-Hirsch, P., Dawsonb, T., and Martin, F., "Diagnostic segregation of human brain tumours using fourier-transform infrared and/or raman spectroscopy coupled with discriminant analysis," *Analytical Methods* **5**, 89–102 (September 2013).

[11] Smitt, M. and Horst, K., "Association of clinical and pathologic variables with lumpectomy surgical margin status after preoperative diagnosis or excisional biopsy of invasive breast cancer," *Annals of Surgical Oncology* **14**, 1040–1044 (March 2007).

[12] Kirsch, M., Schackert, G., Salzer, R., and Krafft, C., "Raman spectroscopic imaging for in vivo detection of cerebral brain metastases," *Analytical and Bioanalytical Chemistry* **398**, 1707–1713 (August 2010).

[13] Diem, M., Mazur, A., Lenau, K., Schubert, J., Bird, B., Miljkovic, M., Krafft, C., and Popp, J., "Molecular pathology via ir and raman spectral imaging," *J. of Biophotonics* **6**, 855–886 (December 2013).

[14] Lu, G. and Fei, B., "Medical hyperspectral imaging: a review," *J. of biomedical optics* **19**, 10901 (January 2014).

[15] Moch, H., Komminoth, P., Zimmermann, D., Odermatt, B., Probst-Hensch, N., and Bopp, M., [*Pathologie*], ch. Pathologie: Aufgaben und Methoden (Kapitel 1), Hrsg.: W. Böcker, H. Denk, Ph.U. Heitz, H. Moch. Elsevier Urban & Fischer, München (2008).

[16] Bhargava, R., "Towards a practical fourier transform infrared chemical imaging protocol for cancer histopathology," *Analytical and Bioanalytical Chemistry* **389**, 1155–1169 (September 2007).

[17] Helenon, O., Correas, J., Balleyguier, C., Ghouadni, M., and Cornud, F., "Ultrasound of renal tumors," *European Radiology* **11**, 1890–1901 (October 2001).

[18] Kramme, R., [*Medizintechnik*], Springer Medizin Verlag, 3 ed. (2007).

[19] Afanasyeva, N., Kolyakov, S., Artioushenko, V., Sokolov, V., and Frank, G., "Minimally invasive and ex-vivo diagnostics of breast cancer tissues by fiber optic evanescent-wave fourier transform ir (few-ftir) spectroscopy," *Proc. SPIE 3250, Optical Biopsy II, San Jose, CA, USA* **3250**, 140–147 (April 1998).

[20] Wu, J., Xu, Y., Sun, C., Soloway, R., Xu, D., Wu, Q., Sun, K., Weng, S., and Xu, G., "Distinguishing malignant from normal oral tissues using ftir fiber-optic techniques," *Biopolymers* **62**(4), 185–192 (2001).

[21] Bindig, U., Wäsche, W., Zelianos, K., and Müller, G., "Fiber-optical and microscopic detection of malignant tissue by use of infrared spectrometry," *Biomedical Optics* **7**, 100–108 (Januar 2002).

[22] Bindig, U., Frank, F., Gersonde, I., Meinke, M., Zelianeos, K., Katzir, A., and Müller, G., "Fiber-optic and microscopic infrared biodiagnostics," *Laser Physics* **13**(1), 96–105 (2003).

[23] Bindig, U., Gersonde, I., Meinke, M., Becker, Y., and Müller, G., "Fibre-optic ir-spectroscopy for biomedical diagnostics," *Spectroscopy: An Int. J.* **17**(2/3), 323–344 (2003).

[24] Heise, H., Kuepper, L., Pittermann, W., and Stuecker, M., "Epidermal in vivo and in vitro studies by attenuated total reflection mid-infrared spectroscopy using flexible silver halide fibre-probes," *J. of Molecular Structure* **651–653**, 127–132 (June 2003).

[25] Li, Q.-B., Xu, Z., Zhang, N.-W., Zhang, L., Wang, F., Yang, L.-M., Wang, J.-S., Zhou, S., Zhang, Y.-F., Zhou, X.-S., Shi, J.-S., and J.-G., W., "In vivo and in situ detection of colorectal cancer using fourier transform infrared spectroscopy," *World J. of Gastroenterology* **11**, 327–330 (Januar 2005).

[26] Mackanos, M. and Contag, C., "Fiber-optic probes enable cancer detection with ftir spectroscopy," *Trends in Biotechnology* **28**, 317–323 (June 2010).

[27] Liu, Y., Xu, Y., Liu, Y., Zhang, Y., Wang, D., Xiu, D., Xu, Z., Zhou, X., Wu, J., and Ling, X., "Detection of cervical metastatic lymph nodes in papillary thyroid carcinoma by fourier transform infrared spectroscopy," *British J. of Surgery* **98**, 380–384 (March 2011).

[28] Steiner, G. and Kirsch, M., "Optical spectroscopic methods for intraoperative diagnosis," *Analytical and Bioanalytical Chemistry* **406**, 21–25 (January 2014).

[29] Yao, H., Shi, X., and Zhang, Y., "The use of ftir-atr spectrometry for evaluation of surgical resection margin in colorectal cancer: A pilot study of 56 samples," *J. of Spectroscopy* **2014, Article ID 213890**, 1–4 (2011).

[30] Yano, K., Ohoshima, S., Gotou, Y., Kumaido, K., Moriguchi, T., and Katayama, H., "Direct measurement of human lung cancerous and noncancerous tissues by fourier transform infrared microscopy: Can an infrared microscope be used as a clinical tool?," *Analytical Biochemistry* **287**, 218–225 (Dezember 2000).

[31] Lasch, P., Haensch, W., Lewis, E., Kidder, L., and Naumann, D., "Characterization of colorectal adenocarcinoma sections by spatially resolved ft-ir microspectroscopy," *Appl. Spectroscopy* **56**(1), 1–9 (2002).

[32] Chang, J.-I., Huang, Y.-B., Wu, P.-C., Chen, C.-C., Huang, S.-C., and Tsaib, Y.-H., "Characterization of human cervical precancerous tissue through the fourier transform infrared microscopy with mapping method," *Gynecologic Oncology* **91**(3), 577–583 (2003).

[33] Gazi, E., Dwyer, J., P., G., Ghanbari-Siahkali, A., Wade, A., Miyan, J., Lockyer, N., Vickerman, J., Clarke, N., Shanks, J., Scott, L., Hart, C., and Brown, M., "Applications of fourier transform infrared microspectroscopy in studies of benign prostate and prostate cancer. a pilot study.," *J. of Pathology* **201**, 99–108 (September 2003).

[34] Steiner, G., Shaw, A., Choo-Smith, L., Abuid, M., Schackert, G., Sobottka, S., Steller, W., Salzer, R., and Mantsch, H., "Distinguishing and grading human gliomas by ir spectroscopy," *Biopolymers* **72**(6), 464–471 (2003).

[35] Yano, K., Sakamoto, Y., Hirosawa, N., Tonooka, S., Katayama, H., Kumaido, K., and Satomi, A., "Applications of fourier transform infrared spectroscopy, fourier transform infrared microscopy and near-infrared spectroscopy to cancer research," *Spectroscopy* **17**(2–3), 315–321 (2003).

[36] Lasch, P., Wolfgang Haensch, W., Naumann, D., and Diem, M., "Imaging of colorectal adenocarcinoma using ft-ir microspectroscopy and cluster analysis," *Biochimica et Biophysica Acta* **1688**, 176–186 (March 2004).

[37] Wood, B., Chiriboga, L., Yee, H., Quinn, M., McNaughton, D., and Diem, M., "Fourier transform infrared (ftir) spectral mapping of the cervical transformation zone, and dysplastic squamous epithelium," *Gynecologic Oncology* **93**, 59–68 (April 2004).

[38] Beleitesa, C., Steiner, G., Sowab, M., Baumgartner, R., Sobottka, S., Schackertc, G., and Salzer, R., "Classification of human gliomas by infrared imaging spectroscopy and chemometric image processing," *Vibrational Spectroscopy* **38**, 143–149 (July 2005).

[39] Fernandez, D., Bhargava, R., Hewitt, S., and Levin, I., "Infrared spectroscopic imaging for histopathologic recognition," *Nature Biotechnology* **23**, 469–474 (April 2005).

[40] Amharref, N., Beljebbar, A., Dukic, S., Venteo, L., Schneider, L., Pluot, M., Vistelle, R., and Manfait, M., "Brain tissue characterisation by infrared imaging in a rat glioma model," *Biochimica et Biophysica Acta* **1758**, 892–899 (July 2006).

[41] Fabian, H., Thi, N., Eiden, M., Lasch, P., Schmitt, J., and Naumann, D., "Diagnosing benign and malignant lesions in breast tissue sections by using ir-microspectroscopy," *Biochimica et Biophysica Acta* **1758**(7), 874–882 (2006).

[42] Krafft, C., Sobottka, S., Geiger, K., Schackert, G., and Salzer, R., "Classification of malignant gliomas by infrared spectroscopic imaging and linear discriminant analysis," *Analytical and Bioanalytical Chemistry* **387**, 1669–1677 (March 2007).

[43] Beljebbar, A., Amharref, N., Leveques, A., Dukic, S., Venteo, L., Schneider, L., Pluot, M., and Manfait, M., "Modeling and quantifying biochemical changes in c6 tumor gliomas by fourier transform infrared imaging," *Analytical Chemistry* **80**, 8406–8415 (November 2008).

[44] Ali, K., Lu, Y., Christensen, C., May, T., Hyett, C., Griebel, R., Fourney, D., Meguro, K., Resch, L., and Sharma, R., "Fourier transform infrared spectromicroscopy and hierarchical cluster analysis of human meningiomas," *Int. J. of Molecular Medicine* **21**, 297–301 (March 2008).

[45] Bird, B., Bedrossian, K., Laver, N., Miljkovic, M., Romeo, M., and Diem, M., "Detection of breast micrometastases in axillary lymph nodes by infrared micro-spectral imaging," *Analyst* **134**, 1067–1076 (April 2009).

[46] Sobottka, S., Geiger, K., Salzer, R., Schackert, G., and Krafft, C., "Suitability of infrared spectroscopic imaging as an intraoperative tool in cerebral glioma surgery," *Analytical and Bioanalytical Chemistry* **393**, 187–195 (January 2009).

[47] Benard, A., Desmedt, C., Durbecq, V., Rouas, G., Larsimont, D., Sotiriou, C., and Goormaghtigh, E., "Discrimination between healthy and tumor tissues on formalin-fixed paraffin-embedded breast cancer samples using ir imaging," *Spectroscopy* **24**(1–2), 67–72 (2010).

[48] Travo, A., Piot, O., Wolthuis, R., Gobinet, C., Manfait, M., Bara, J., Forgue-Lafitte, M., and Jeannesson, P., "Ir spectral imaging of secreted mucus: a promising new tool for the histopathological recognition of human colonic adenocarcinomas," *Histopathology* **56**, 921–931 (June 2010).

[49] Nasse, M., Walsh, M., Mattson, E., Reininger, R., Kajdacsy-Balla, A., Macias, V., Bhargava, R., and Hirschmugl, C., "High-resolution fourier-transform infrared chemical imaging with multiple synchrotron beams," *Nature Methods* **8**, 413–416 (March 2011).

[50] Bird, B., Miljkovic, M., Remiszewski, S., Akalin, A., Kon, M., and Diem, M., "Infrared spectral histopathology (shp): a novel diagnostic tool for the accurate classification of lung cancer," *Laboratory Investigation* **92**, 1358–1373 (September 2012).

[51] Nallala, J., Piot, O., Diebold, M., Gobinet, C., Bouche, O., Manfait, M., and Sockalingum, G., "Infrared imaging as a cancer diagnostic tool: introducing a new concept of spectral barcodes for identifying molecular changes in colon tumors," *Cytometry A* **83**, 294–300 (March 2013).

[52] Das, K., Kendall, C., Isabelle, M., Fowler, C., Christie-Brown, J., and Stone, N., "Ftir of touch imprint cytology: a novel tissue diagnostic technique," *J. of Photochemistry and Photobiology B* **92**, 160–164 (September 2008).

[53] Siebert, F. and Hildebrandt, P., [*Vibrational Spectroscopy in Life Science*], Wiley-VCH Verlag, 1 ed. (2008).

[54] Griffiths, P. and De Haseth, J., [*Fourier Transform Infrared Spectrometry*], Chemical Analysis: A Series of Monographs on Analytical Chemistry and Its Applications, John Wiley & Sons, 2 ed. (April 2007).

[55] Fahrenfort, J., "A new principle for the production of useful infra-red reflection spectra of organic compounds," *Spectrochimica Acta* **17**(7), 698–709 (1961).

[56] Kazarian, S. and Chan, K., "Micro- and macro- attenuated total reflection fourier transform infrared spectroscopic imaging," *Appl. Spectroscopy* **64**, 135A–152A (May 2010).

[57] Milosevic, M., [*Internal Reflection and ATR Spectroscopy*], Chemical Analysis: A Series of Monographs on Analytical Chemistry and Its Applications, John Wiley & Sons, 1 ed. (Juni 2012).

[58] Pleitez, M., von Lilienfeld-Toal, H., and Maentele, W., "Infrared spectroscopic analysis of human interstitial fluid in vitro and in vivo using ft-ir spectroscopy and pulsed quantum cascade lasers (qcl): Establishing a new approach to non invasive glucose measurement," *Spectrochimica Acta Part A: Molecular and Biomolecular Spectroscopy* **85**, 61–65 (January 2012).

[59] Brandstetter, M., Sumalowitsch, T., Genner, A., Posch, A., Herwig, C., Drolz, A., Fuhrmann, V., Perkmann, T., and Lendl, B., "Reagent-free monitoring of multiple clinically relevant parameters in human blood plasma using a mid-infrared quantum cascade laser based sensor system," *Analyst* **138**, 4022–4028 (July 2013).

[60] Bassan, P., Weida, M., Rowlette, J., and Gardner, P., "Large scale infrared imaging of tissue micro arrays (tmas) using a tunable quantum cascade laser (qcl) based microscope," *Analyst* **139**, 3856–3859 (August 2014).

[61] Kroeger, N., Egl, A., Engel, M., Gretz, N., Haase, K., Herpich, I., Kraenzlin, B., Neudecker, S., Pucci, A., Schoenhals, A., Vogt, J., and Petrich, W., "Quantum cascade laser-based hyperspectral imaging of biological tissue," *J. of biomedical optics* **19**, 111607 (November 2014).

[62] Levin, W. and Bhargava, R., "Fourier transform infrared vibrational spectroscopic imaging: integrating microscopy and molecular recognition," *Annual Review of Physical Chemistry* **56**, 429–474 (2005).

[63] Jackson, M., Choo, L., Watson, P., Halliday, W., and Mantsch, H., "Beware of connective tissue proteins: assignment and implications of collagen absorptions in infrared spectra of human tissues," *Biochimica et Biophysics Acta* **1270**, 1–6 (January 1995).

[64] Wong, P., Papavassiliou, E., and Rigas, B., "Phosphodiester stretching bands in the infrared spectra of human tissues and cultured cells," *Appl. Spectroscopy* **45**, 1563–1567 (September 1991).

[65] Movasaghi, Z., Rehman, S., and Rehman, I., "Fourier transform infrared (ftir) spectroscopy of biological tissues," *Applied Spectroscopy Reviews* **43**, 134–179 (February 2008).